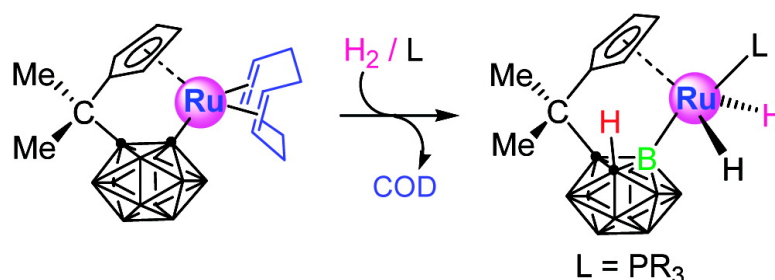


Hydrogen-Mediated Metal#Carbon to Metal#Boron Bond Conversion in Metal#Carboranyl Complexes

Dongmei Liu, Li Dang, Yi Sun, Hoi-Shan Chan, Zhenyang Lin, and Zuwei Xie

J. Am. Chem. Soc., **2008**, 130 (47), 16103-16110 • DOI: 10.1021/ja8067098 • Publication Date (Web): 31 October 2008

Downloaded from <http://pubs.acs.org> on February 8, 2009



More About This Article

Additional resources and features associated with this article are available within the HTML version:

- Supporting Information
- Access to high resolution figures
- Links to articles and content related to this article
- Copyright permission to reproduce figures and/or text from this article

[View the Full Text HTML](#)

Hydrogen-Mediated Metal–Carbon to Metal–Boron Bond Conversion in Metal–Carboranyl Complexes

Dongmei Liu,[†] Li Dang,[‡] Yi Sun,^{†,§} Hoi-Shan Chan,[†] Zhenyang Lin,^{*,‡} and Zuowei Xie^{*,†}

Departments of Chemistry, The Chinese University of Hong Kong, Shatin, New Territories, Hong Kong, China, and The Hong Kong University of Science and Technology, Clear Water Bay, Kowloon, Hong Kong, China

Received August 25, 2008; E-mail: zxie@cuhk.edu.hk

Abstract: A hydrogen-mediated Ru–C to Ru–B bond conversion was observed experimentally and supported by the theoretical calculations. Treatment of [$\eta^5\text{-}\sigma\text{-C-Me}_2\text{C}(\text{C}_5\text{H}_4)(\text{C}_2\text{B}_{10}\text{H}_{10})$]Ru(COD) (**1**) bearing a Ru–C(cage) σ bond with PR_3 in the presence of H_2 gave Ru–B(cage) bonded complexes [$\eta^5\text{-}\sigma\text{-B-Me}_2\text{C}(\text{C}_5\text{H}_4)(\text{C}_2\text{B}_{10}\text{H}_{10})$]RuH₂(PR_3) (R = Cy (**2**), Ph (**3**)) ($\sigma\text{-C}$: Ru–C(cage) σ bond; $\sigma\text{-B}$: Ru–B(cage) σ bond). Complex **3** was converted to [$\eta^5\text{-}\sigma\text{-B-Me}_2\text{C}(\text{C}_5\text{H}_4)(\text{C}_2\text{B}_{10}\text{H}_{10})$]Ru(L₂) in the presence of L₂ (L₂ = dppe (**4**), PPh₃/P(OEt)₃ (**5**), PPh₃/pyridine (**6**)) via liberation of H_2 upon heating. These complexes were fully characterized by various spectroscopic techniques, elemental analyses, and single-crystal X-ray diffraction studies. DFT calculations show that this conversion process is both kinetically and thermodynamically favorable and requires involvement of a hydride ligand.

Introduction

It is well-established that *o*-carboranes can be readily converted to the monoanion *closo*-C₂B₁₀H₁₁[−] and dianion *closo*-C₂B₁₀H₁₀^{2−} via stepwise deprotonation of the cage C–H protons,¹ the dicarbollide ion (*nido*-C₂B₉H₁₁^{2−}) by selective removal of one BH vertex,² the *nido*-C₂B₁₀H₁₂^{2−} and *arachno*-C₂B₁₀H₁₂^{4−} through reaction with group 1 metals.^{3,4} These anionic ligands can bond to d- and f-block transition metal ions in a σ -, η^5 -, η^6 -, and η^7 -fashion, respectively, constituting a very rich and versatile coordination chemistry. As a result, a large

number of metal–carboranyl and metallocarborane complexes have been prepared and extensively investigated.^{5,6}

Reactivity studies show that significantly different from metal–carbon σ bonds in metal alkyls and metal aryls,⁷ the metal–carbon(cage) σ bond in metal–carboranyl complexes is

[†] The Chinese University of Hong Kong.

[‡] The Hong Kong University of Science and Technology.

[§] Current address: Department of Chemistry, Queen's University, Kingston, Ontario K7L 3N6, Canada.

- (1) (a) Boone, J. L.; Brotherton, R. J.; Petterson, L. L. *Inorg. Chem.* **1965**, *4*, 910. (b) Heying, T. L.; Ager, J. W.; Clark, S. L.; Alexander, R. P.; Papetti, S.; Reid, J. A.; Trotz, S. I. *Inorg. Chem.* **1963**, *2*, 1097. (c) Stanko, V. I.; Klimova, A. I. *Zh. Obshch. Khim.* **1965**, *35*, 1141.
- (2) (a) Wiesboeck, R. A.; Hawthorne, M. F. *J. Am. Chem. Soc.* **1964**, *86*, 1642. (b) Hawthorn, M. F.; Wegner, P. A.; Stafford, R. C. *Inorg. Chem.* **1965**, *4*, 1675. (c) Dunks, G. B.; Hawthorne, M. F. *Acc. Chem. Res.* **1973**, *6*, 124. (d) Nöth, H.; Vahrenkamp, H. *Chem. Ber.* **1966**, *99*, 1049. (e) Füssstetter, H.; Nöth, H.; Wrackmeyer, B.; McFarlane, W. *Chem. Ber.* **1977**, *110*, 3172. (f) Wei, X.; Carroll, P. J.; Sneddon, L. G. *Organometallics* **2006**, *25*, 609. (g) Yoo, J.; Hwang, J.-W.; Do, Y. *Inorg. Chem.* **2001**, *40*, 568. (h) Teixidor, F.; Gómez, S.; Lamrani, M.; Viñas, C.; Sillanpää, R.; Kivekäs, R. *Organometallics* **1997**, *16*, 1278. (i) Shen, H.; Chan, H.-S.; Xie, Z. *Organometallics* **2008**, *27*, 1157. (j) Lee, Y.-J.; Lee, J.-D.; Ko, J.; Kim, S.-H.; Kang, S. O. *Chem. Commun.* **2003**, 1364. (k) Teixidor, F.; Viñas, C.; Benakki, R.; Kivekäs, R.; Sillanpää, R. *Inorg. Chem.* **1997**, *36*, 1719.
- (3) (a) Dunks, G. B.; Wiersema, R. J.; Hawthorne, M. F. *J. Am. Chem. Soc.* **1973**, *95*, 3174. (b) Tolpin, E. I.; Lipscomb, W. N. *Inorg. Chem.* **1973**, *12*, 2257. (c) Churchill, M. R.; DeBoer, B. G. *Inorg. Chem.* **1973**, *12*, 2674. (d) Chui, K.; Li, H.-W.; Xie, Z. *Organometallics* **2000**, *19*, 5447.
- (4) (a) Evans, W. J.; Hawthorne, M. F. *J. Chem. Soc., Chem. Commun.* **1974**, 38. (b) Ellis, D.; Lopez, M. E.; McIntosh, R.; Rosair, G. M.; Welch, A. J. *Chem. Commun.* **2005**, 1917.

- (5) (a) Hawthorne, M. F.; Owen, D. A.; Smart, J. C.; Garrett, P. M. *J. Am. Chem. Soc.* **1971**, *93*, 1362. (b) Smart, J. C.; Garrett, P. M.; Hawthorne, M. F. *J. Am. Chem. Soc.* **1969**, *91*, 1031. (c) Zakharkin, L. I.; Orlova, L. V.; Denisovich, L. I. *Zh. Obshch. Khim.* **1972**, *42*, 2217. (d) Bresadola, S.; Cecchin, G.; Turco, A. *Gazz. Chim. Ital.* **1970**, *100*, 682. (e) Bresadola, S.; Rigo, P.; Turco, A. *J. Chem. Soc., Chem. Commun.* **1968**, 1205. (f) Bresadola, S.; Frigo, A.; Longato, B.; Rigatti, G. *Inorg. Chem.* **1973**, *12*, 2788. (g) Bresadola, S.; Longato, B.; Morandini, F. *J. Organomet. Chem.* **1977**, *128*, C5. (h) Bresadola, S.; Bresciani-Pahor, N.; Longato, B. *J. Organomet. Chem.* **1979**, *179*, 73. (i) Bresadola, S.; Longato, B.; Morandini, F. *J. Chem. Soc., Chem. Commun.* **1974**, 510. (j) Allegra, G.; Calligaris, M.; Furlanetto, R.; Nardin, G.; Randaccio, L. *Cryst. Struct. Commun.* **1974**, *3*, 69. (k) Longato, B.; Morandini, F.; Bresadola, S. *Inorg. Chem.* **1976**, *15*, 650. (l) Owen, D. A.; Hawthorne, M. F. *J. Am. Chem. Soc.* **1970**, *92*, 3194. (m) Love, R. A.; Bau, R. *J. Am. Chem. Soc.* **1972**, *94*, 8274. (n) Hawthorne, M. F.; Zheng, Z. P. *Acc. Chem. Res.* **1997**, *30*, 267.
- (6) For reviews, see: (a) Deng, L.; Xie, Z. *Organometallics* **2007**, *26*, 1832. (b) Deng, L.; Xie, Z. *Coord. Chem. Rev.* **2007**, *251*, 2452. (c) Xie, Z. *Coord. Chem. Rev.* **2006**, *250*, 259. (d) Hosmane, N. S.; Maguire, J. A. *Organometallics* **2005**, *24*, 1356. (e) Krossing, I.; Raabe, I. *Angew. Chem., Int. Ed.* **2004**, *43*, 2066. (f) Hosmane, N. S.; Maguire, J. A. *Eur. J. Inorg. Chem.* **2003**, *22*, 3989. (g) Wedge, T. J.; Hawthorne, M. F. *Coord. Chem. Rev.* **2003**, *240*, 111. (h) Xie, Z. *Acc. Chem. Res.* **2003**, *36*, 1. (i) Xie, Z. *Coord. Chem. Rev.* **2002**, *231*, 23. (j) Valliant, J. F.; Guenther, K. J.; King, A. S.; Morel, P.; Schaffer, P.; Sogbein, O. O.; Stephenson, K. A. *Coord. Chem. Rev.* **2000**, *232*, 173. (k) Grimes, R. N. *Coord. Chem. Rev.* **2000**, *200*, 773. (l) Saxena, A. K.; Maguire, J. A.; Hosmane, N. S. *Chem. Rev.* **1997**, *97*, 2421. (m) Saxena, A. K.; Hosmane, N. S. *Chem. Rev.* **1993**, *93*, 1081. (n) Hosmane, N. S.; Maguire, J. A. In *Comprehensive Organometallic Chemistry III*; Crabtree, R. H., Mingos, D. M. P., Eds; Elsevier: Oxford, 2007; Vol. 3, p175. (o) Grimes, R. N. In *Comprehensive Organometallic Chemistry II*; Abel, E. W., Stone, F. G. A., Wilkinson, G., Eds; Pergamon: New York, 1995; Vol. 1, p 373.

inert toward various unsaturated molecules.^{6c,g,8} For instance, the following relative reactivity is observed in $[\eta^5\text{-}\sigma\text{-Me}_2\text{C}(\text{C}_5\text{H}_4)(\text{C}_2\text{B}_{10}\text{H}_{10})]\text{TiR}(\text{NMe}_2)$: $\text{Ti}-\text{C}(\text{alkyl}) > \text{Ti}-\text{N} \gg \text{Ti}-\text{C}(\text{cage})$, although the distances of $\text{Ti}-\text{C}(\text{alkyl})$ and $\text{Ti}-\text{C}(\text{cage})$ are almost identical.⁹ The $\text{Zr}-\text{C}(\text{cage})$ bond in $[\eta^5\text{-}\sigma\text{-Me}_2\text{A}(\text{C}_9\text{H}_6)(\text{C}_2\text{B}_{10}\text{H}_{10})]\text{Zr}(\text{NMe}_2)_2$ ($\text{A} = \text{C}, \text{Si}$) does not show any activity toward unsaturated molecules.^{8c-i} Alkynes do not insert into the $\text{Ru}-\text{C}(\text{cage})$ σ bond in $[\eta^5\text{-}\sigma\text{-Me}_2\text{C}(\text{C}_5\text{H}_4)(\text{C}_2\text{B}_{10}\text{H}_{10})]\text{Ru}(\text{CH}_3\text{CN})_2$.¹⁰ Alkynes and alkenes do not react with the $\text{Ni}-\text{C}(\text{cage})$ σ bond either.¹¹ The inertness of such metal–carbon(cage) σ bonds can be probably ascribed to the presence of a sterically demanding icosahedral cage which protects the metal–carbon bond from attack of electrophiles.^{8e,9,10} These results may lead one to believe that the prevalent $\text{M}-\text{C}$ σ -bonded metal–carboranyl complexes reported in the literature are likely thermodynamic products.

We have recently discovered an unprecedented transformation of the $\text{Ru}-\text{C}(\text{cage})$ σ bond to the $\text{Ru}-\text{B}(\text{cage})$ σ bond in the presence of dihydrogen gas during the course of hydrogenolysis of $[\eta^5\text{-}\sigma\text{-Me}_2\text{C}(\text{C}_5\text{H}_4)(\text{C}_2\text{B}_{10}\text{H}_{10})]\text{Ru}(\text{COD})$. DFT calculations show that this process is both kinetically and thermodynamically favorable and dihydrogen plays a key role in this transformation. These findings are reported in this article.

Results and Discussion

$[\eta^5\text{-}\sigma\text{-Me}_2\text{C}(\text{C}_5\text{H}_4)(\text{C}_2\text{B}_{10}\text{H}_{10})]\text{RuH}_2(\text{PR}_3)$. It has been reported that the $\text{Ru}-\text{C}(\text{cage})$ σ -bonded complex $[\eta^5\text{-}\sigma\text{-Me}_2\text{C}(\text{C}_5\text{H}_4)(\text{C}_2\text{B}_{10}\text{H}_{10})]\text{Ru}(\text{COD})$ (**1**) (σC : $\text{Ru}-\text{C}(\text{cage})$ σ bond) does not react with PCy_3 ($\text{Cy} = \text{cyclohexyl}$) or PPh_3 even at refluxing THF probably due to steric reasons.¹² However, in the presence of H_2 , **1** reacted readily with PR_3 in THF at 60 °C to give the $\text{Ru}-\text{B}(\text{cage})$ σ -bonded dihydride complexes $[\eta^5\text{-}\sigma\text{-Me}_2\text{C}(\text{C}_5\text{H}_4)(\text{C}_2\text{B}_{10}\text{H}_{10})]\text{RuH}_2(\text{PR}_3)$ (σB : $\text{Ru}-\text{B}(\text{cage})$ σ bond; $\text{R} = \text{Cy}$ (**2**), Ph (**3**)) in 87–88% isolated yields (Scheme 1). They are very sensitive to air and moisture, but remain stable under inert atmosphere for months. Both **2** and **3** are soluble in THF and aromatic solvents but are insoluble in hexane.

In addition to the resonances of Me_2C and PCy_3 (in **2**) or PPh_3 (in **3**) protons, four multiplets in the range of 5.26–4.18 ppm corresponding to the protons of cyclopentadienyl ring, one characteristic broad singlet at ca. 3.30 ppm assignable to the cage CH proton and one doublet of doublet at -10.58 ppm with

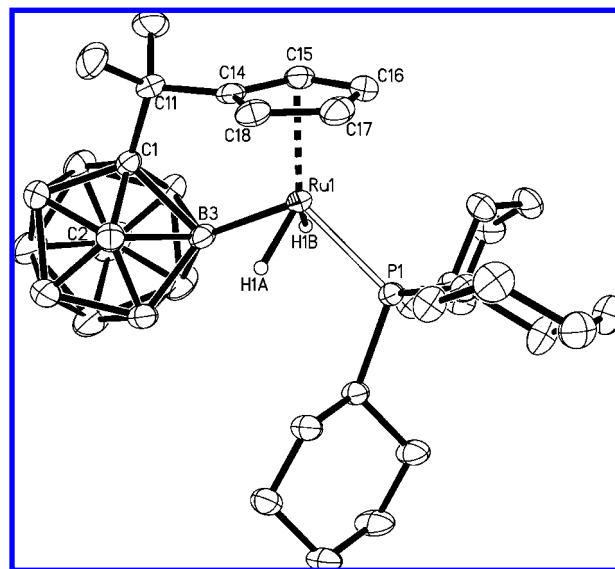
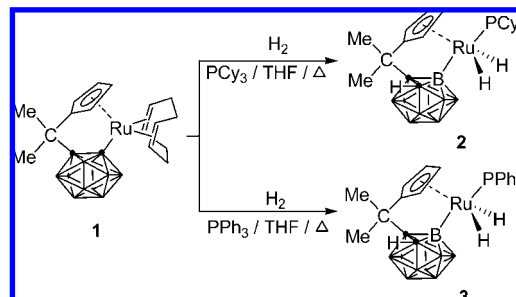


Figure 1. Molecular structure of $[\eta^5\text{-}\sigma\text{-Me}_2\text{C}(\text{C}_5\text{H}_4)(\text{C}_2\text{B}_{10}\text{H}_{10})]\text{RuH}_2\text{PCy}_3$ (**2**) (thermal ellipsoids drawn at the 30% probability level).

Scheme 1



$^2J_{\text{PH}} = 30.0$ Hz and $^2J_{\text{HH}} = 3.0$ Hz in **2** and -9.6 ppm with $^2J_{\text{PH}} = 30.0$ Hz and $^2J_{\text{HH}} = 3.0$ Hz in **3** attributable to the $\text{Ru}-\text{H}_2$ hydrido protons, were observed in the ^1H NMR spectra. The ^{13}C NMR data were consistent with the ^1H NMR results. The $^{11}\text{B}\{^1\text{H}\}$ NMR spectra showed a 1:1:1:2:2:2:1 pattern for **2** and a 1:1:1:1:2:3:1 pattern for **3**. The proton-coupled ^{11}B NMR exhibited clearly a singlet at 10.75 ppm for **2** and at 9.37 ppm for **3**, indicating that no proton is bonded to this boron atom. The above spectroscopic data suggested that the Ru atom may be bonded to the cage B rather than the cage C atom. The ^{31}P NMR spectra displayed one signal at 82.2 ppm for **2** and 51.3 ppm for **3**. The characteristic $\text{Ru}-\text{H}$ absorption at 1958 cm^{-1} in **2** and 1990 cm^{-1} in **3** was also observed in the solid-state IR spectra.¹³ Their compositions were confirmed by elemental analyses.

Single-crystal X-ray diffraction studies revealed that the Ru atom is η^5 -bound to the cyclopentadienyl ring, σ -bound to one cage boron atom and two hydrogen atoms, and coordinated to one P atom in a four-legged piano stool geometry. Figures 1 and 2 show the molecular structures of **2** and **3**, respectively. Table 1 summarizes the selected bond distances and angles. The $\text{Ru}-\text{B}(\text{cage})$ distances of 2.075(3)/2.087(3) Å in **2** and **3** are very comparable to that of 2.110(1) Å in *transoid*-(*p*-cyme-

(7) For reviews, see: (a) Schrock, R. R.; Parshall, G. W. *Chem. Rev.* **1976**, *76*, 243. (b) Cotton, F. A. *Chem. Rev.* **1957**, *55*, 551. (c) Newkome, G. R.; Puckett, W. E.; Gupta, V. K.; Kiefer, G. E. *Chem. Rev.* **1986**, *86*, 451.

(8) (a) Usatov, A. V.; Martynova, E. V.; Dolgushin, F. M.; Peregudov, A. S.; Antipin, M. Y.; Novikov, Y. N. *Eur. J. Inorg. Chem.* **2002**, 2565. (b) Usatov, A. V.; Martynova, E. V.; Dolgushin, F. M.; Peregudov, A. S.; Antipin, M. Y.; Novikov, Y. N. *Eur. J. Inorg. Chem.* **2003**, 29. (c) Wang, X.; Jin, G.-X. *Chem.-Eur. J.* **2005**, *11*, 5758. (d) Wang, X.; Jin, G.-X. *Organometallics* **2004**, *23*, 6319. (e) Wang, H.; Li, H.-W.; Xie, Z. *Organometallics* **2003**, *22*, 4522. (f) Wang, Y.; Wang, H.; Wang, H.; Chan, H.-S.; Xie, Z. *J. Organomet. Chem.* **2003**, *683*, 39. (g) Wang, H.; Wang, H.; Li, H.-W.; Xie, Z. *Organometallics* **2004**, *23*, 875. (h) Wang, H.; Chan, H.-S.; Xie, Z. *Organometallics* **2005**, *24*, 3772. (i) Deng, L.; Chan, H.-S.; Xie, Z. *J. Am. Chem. Soc.* **2005**, *127*, 13774.

(9) Wang, H.; Wang, Y.; Chan, H.-S.; Xie, Z. *Inorg. Chem.* **2006**, *45*, 5675.

(10) (a) Sun, Y.; Chan, H.-S.; Zhao, H.; Lin, Z.; Xie, Z. *Angew. Chem., Int. Ed.* **2006**, *45*, 5533. (b) Sun, Y.; Chan, H.-S.; Dixneuf, P. H.; Xie, Z. *Organometallics* **2006**, *25*, 2719.

(11) (a) Deng, L.; Chan, H.-S.; Xie, Z. *J. Am. Chem. Soc.* **2006**, *128*, 7728. (b) Qiu, Z.; Xie, Z. *Angew. Chem., Int. Ed.* **2008**, *47*, 6572.

(12) Sun, Y.; Chan, H.-S.; Dixneuf, P. H.; Xie, Z. *Organometallics* **2004**, *23*, 5864.

(13) These data are similar to those reported in the following literature: Abdur-Rashid, K.; Abbel, R.; Hadzovic, A.; Lough, A. J.; Morris, R. H. *Inorg. Chem.* **2005**, *44*, 2483.

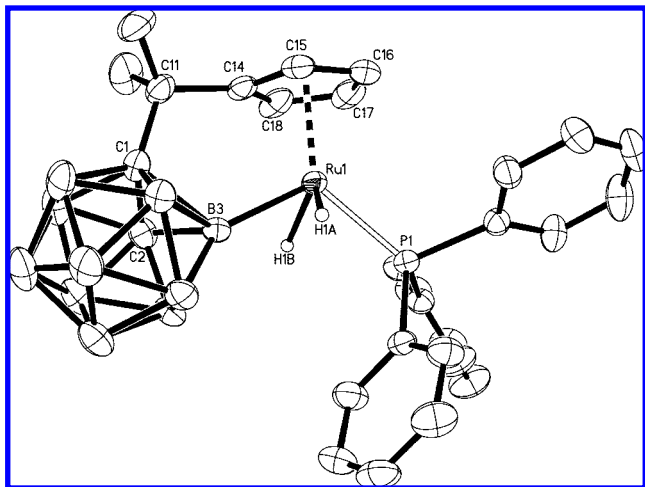


Figure 2. Molecular structure of $[\eta^5\text{-}\sigma\text{-Me}_2\text{C}(\text{C}_5\text{H}_4)(\text{C}_2\text{B}_{10}\text{H}_{10})]\text{RuH}_2\text{PPh}_3$ (**3**) (thermal ellipsoids drawn at the 30% probability level).

$\text{neRu}\{\sigma\text{-}\sigma\text{-}\sigma\text{-}\text{SS}(\text{HCCH})\text{C}_2\text{B}_{10}\text{H}_{10}\}$,¹⁴ 2.100(3) Å in $\text{Ru}(\text{Bcat})_2(\text{CO})_2(\text{PPh}_3)_2$,¹⁵ and 2.093(3) Å in $\text{Ru}(\text{Bcat})_2(\text{CO})(\text{CN-}p\text{-tolyl})(\text{PPh}_3)_2$.¹⁵ The average Ru–C(ring) distances of 2.249(2)/2.239(3) Å in **2/3** are close to that of 2.230(4) Å in **1** and 2.263(2) Å in $[\eta^5\text{-Me}_2\text{C}(\text{C}_5\text{H}_3)(\text{C}_2\text{B}_{10}\text{H}_{10})]\text{RuH}(\text{PPh}_3)_2$.¹⁶ The Ru–Cent distances of 1.898/1.887 Å in **2/3** are very similar to that of 1.910 Å in $[\eta^5\text{-Me}_2\text{C}(\text{C}_5\text{H}_3)(\text{C}_2\text{B}_{10}\text{H}_{10})]\text{RuH}(\text{PPh}_3)_2$,¹⁶ 1.907 Å in $[\eta^5\text{-C}_5\text{D}_4(\text{MeC}_2\text{B}_{10}\text{H}_{10})]\text{RuD}(\text{PPh}_3)_2$,¹⁷ 1.881 Å in $(\text{Cp})(\text{MeC}_2\text{B}_{10}\text{H}_{10})\text{Ru}(\text{PMe}_2\text{Ph})_2$,¹⁸ and 1.889 Å in $\text{CpRuH}(\text{PPh}_3)_2$.¹⁹ The average Ru–H distances of 1.44(3)/1.52(3) Å in **2/3** compare to that of 1.55(2) Å (Ru–D distance) in $[\eta^5\text{-C}_5\text{D}_4(\text{MeC}_2\text{B}_{10}\text{H}_{10})]\text{RuD}(\text{PPh}_3)_2$,¹⁷ 1.54(1) Å in $[\eta^5\text{-Me}_2\text{C}(\text{C}_5\text{H}_3)(\text{C}_2\text{B}_{10}\text{H}_{10})]\text{RuH}(\text{PPh}_3)_2$,¹⁶ 1.55(3) Å in $(\text{C}_3\text{H}_4\text{CH}_2\text{CH}_2\text{-NMe}_2)\text{RuH}(\text{PPh}_3)_2$,²⁰ and 1.51(4) Å in $\text{CpRuH}(\text{PPh}_3)_2$.¹⁹ The Cent–Ru–B(cage) angles of 114.6/114.1° in **2/3** are slightly larger than the Cent–Ru–C(cage) angle of 111.8° in **1** and the Cent–Ru–Cl angle of 112.2° in $\text{Cp}^*\text{RuCl}(\text{COD})$.²¹ The $\text{C}_{\text{ring}}\text{-C}_{\text{bridge}}\text{-B}_{\text{cage}}$ angles of 109.0(2)/109.4(2)° in **2/3** are comparable to the $\text{C}_{\text{ring}}\text{-C}_{\text{bridge}}\text{-C}_{\text{cage}}$ angles of 108–120° observed in $[\eta^5\text{-}\sigma\text{-Me}_2\text{C}(\text{C}_5\text{H}_4)(\text{C}_2\text{B}_{10}\text{H}_{10})]\text{Ru}(\text{L}_2)$ (L_2 = bidentate phosphines, bipyridine, phosphites, amines, nitriles, bidentate amines, and amines/phosphines).^{12,22}

$[\eta^5\text{-}\sigma\text{-Me}_2\text{C}(\text{C}_5\text{H}_4)(\text{C}_2\text{B}_{10}\text{H}_{10})]\text{Ru}(\text{L}_2)$. In the presence of a coordinating ligand, $[\eta^5\text{-}\sigma\text{-Me}_2\text{C}(\text{C}_5\text{H}_4)(\text{C}_2\text{B}_{10}\text{H}_{10})]\text{RuH}_2(\text{PPh}_3)$ (**3**) was readily converted to $[\eta^5\text{-}\sigma\text{-Me}_2\text{C}(\text{C}_5\text{H}_4)(\text{C}_2\text{B}_{10}\text{H}_{10})]\text{-Ru}(\text{L}_2)$ in high yields (L_2 = dppe (1,2-bis(diphenylphosphino)ethane) (**4**), $\text{PPh}_3/\text{P}(\text{OEt})_3$ (**5**), $\text{PPh}_3/\text{pyridine}$ (**6**)) upon heating in toluene through liberation of dihydrogen, as shown in Scheme 2.

- (14) Herberhold, M.; Yan, H.; Milius, W.; Wrackmeyer, B. *Chem.–Eur. J.* **2002**, *8*, 388.
 (15) Rickard, C. E. F.; Roper, W. R.; Williamson, A.; Wright, L. J. *Organometallics* **2000**, *19*, 4344.
 (16) Sun, Y.; Chan, H.-S.; Dixneuf, P. H.; Xie, Z. *Chem. Commun.* **2004**, 2588.
 (17) Basato, M.; Biffis, A.; Tubaro, C.; Graiff, C.; Tiripicchio, A. *Dalton Trans.* **2004**, 4092.
 (18) Basato, M.; Biffis, A.; Buscemi, G.; Callegaro, E.; Polo, M.; Tubaro, C.; Venzo, A.; Vianini, C.; Graiff, C.; Tiripicchio, A.; Benetollo, F. *Organometallics* **2007**, *26*, 4265.
 (19) Smith, K.-T.; Rømming, C.; Tilsset, M. *J. Am. Chem. Soc.* **1993**, *115*, 8681.
 (20) Ayllon, J. A.; Sayers, S. F.; Sabo-Etienne, S.; Donnadiou, B.; Chaudret, B.; Clot, E. *Organometallics* **1999**, *18*, 3981.
 (21) Serron, S. A.; Luo, L.; Li, C.; Cucullu, M. E.; Stevens, E. D.; Nolan, S. P. *Organometallics* **1995**, *14*, 5290.
 (22) Sun, Y.; Chan, H.-S.; Dixneuf, P. H.; Xie, Z. *J. Organomet. Chem.* **2006**, *691*, 3071.

In addition to the signals assignable to L_2 and $\text{Me}_2\text{C-}$, four multiplets in the range of 5.46–3.35 ppm attributable to the Cp ring protons and a characteristic broad singlet at 2.35 ppm in **4**, 3.12 ppm in **5**, and 2.52 ppm in **6** corresponding to the cage CH proton were observed in the ^1H NMR spectra. Their ^{13}C NMR data were consistent with the above results. The $^{11}\text{B}\{^1\text{H}\}$ NMR spectra showed a pattern of 1:1:1:2:3:1:1 for **4** and 1:1:1:1:3:2:1 for both **5** and **6**. The unique ^{11}B NMR signal of the B atom bonded to the Ru atom was assigned by comparison of the ^1H decoupled and coupled ^{11}B NMR spectra. The chemical shift of this boron was found to be shifted to the lower field, 15.0 ppm in **4**, 15.6 ppm in **5**, and 18.2 ppm in **6**.

Single-crystal X-ray analyses revealed that the Ru atom is η^5 -bound to the cyclopentadienyl ring, σ -bound to one cage boron atom, and coordinated to two P atoms in **4** and **5** or one P atom and one N atom in **6** in a distorted tetrahedral geometry. The structures of **4–6** are shown in Figures 3–5, respectively. The average Ru–C(ring) and Ru–B(cage) distances and the Cent–Ru–B(cage) and $\text{C}_{\text{ring}}\text{-C}_{\text{bridge}}\text{-B}_{\text{cage}}$ angles in **4–6** are similar to each other, as indicated in Table 1. These measured values are also close to those observed in **2** and **3**. The P–Ru–P angle of 95.2(1)° in **5** is much larger than that of 82.3(1)° in **4** but is similar to that of 93.6(1)° in $[\eta^5\text{-}\sigma\text{-Me}_2\text{C}(\text{C}_5\text{H}_4)(\text{C}_2\text{B}_{10}\text{H}_{10})]\text{Ru}[\text{P}(\text{OEt})_3]_2$ ²² and 95.8(1)° in $[\eta^5\text{-}\sigma\text{-Me}_2\text{C}(\text{C}_5\text{H}_4)(\text{C}_2\text{B}_{10}\text{H}_{10})]\text{Ru}[\text{PPh}_2(\text{OEt})]_2$.²² The P–Ru–N angle of 96.3(1)° in **6** is similar to the P–Ru–P angle of 95.2(1)° in **5** but is larger than that of 89.3(2)° in $[\eta^5\text{-}\sigma\text{-Me}_2\text{C}(\text{C}_5\text{H}_4)(\text{C}_2\text{B}_{10}\text{H}_{10})]\text{-Ru}(\text{NH}_2\text{Pr}^n)(\text{PPh}_3)$.²²

We have previously synthesized the Ru–C(cage) σ -bonded complex $[\eta^5\text{-}\sigma\text{-Me}_2\text{C}(\text{C}_5\text{H}_4)(\text{C}_2\text{B}_{10}\text{H}_{10})]\text{Ru}(\text{dppe})$ (**8**)¹² by conventional ligand substitution reaction of $[\eta^5\text{-}\sigma\text{-Me}_2\text{C}(\text{C}_5\text{H}_4)(\text{C}_2\text{B}_{10}\text{H}_{10})]\text{Ru}(\text{COD})$ (**1**) with dppe, which allows a direct comparison between the two closely related isomers **4** and **8** as they are different only in the cage atom bonded to the Ru atom. They showed significant differences in their ^1H , ^{13}C , ^{11}B , and ^{31}P NMR spectra due to changes in molecular symmetry. For example, in the ^1H NMR spectra, two multiplets of the Cp protons and one singlet of the $\text{Me}_2\text{C-}$ unit were found in **8**, whereas four multiplets and two singlets were observed in **4**. The ^{11}B NMR spectra showed a 2:4:4 pattern in **8** and a 1:1:1:2:3:1:1 pattern in **4**. Only one signal at 81.0 ppm was observed in the ^{31}P NMR spectrum of **8**, while two peaks at 89.3 and 87.6 ppm were found in **4**. Single-crystal X-ray analyses indicated that complexes **4** and **8** are isomorphous and isostructural if the differences in cages C and B atoms are ignored. The Cent–Ru–B(cage)/P–Ru–P/ $\text{C}_{\text{ring}}\text{-C}_{\text{bridge}}\text{-B}_{\text{cage}}$ angles of 113.6/82.3(1)/109.1(4)° in **4** are very close to the values of 114.3° (Cent–Ru–C(cage)), 82.1(1)° (P–Ru–P), and 108.5(5)° ($\text{C}_{\text{ring}}\text{-C}_{\text{bridge}}\text{-C}_{\text{cage}}$) observed in **8**. The average Ru–Cent distance of 2.259(6) Å in **4** is slightly longer than that of 2.218(7) Å in **8**. However, the Ru–B(cage) distance of 2.088(6) Å in **4** is much shorter than the Ru–C(cage) distance of 2.141(5) Å in **8**. It is noted that **8** cannot be converted to **4** in the presence of H_2 as **8** does not react with H_2 , suggestive of the importance of formation of ruthenium hydride in the aforementioned Ru–C(cage) to Ru–B(cage) transformation.

$\{[\eta^5\text{-}\sigma\text{-Me}_2\text{C}(\text{C}_5\text{H}_4)(\text{C}_2\text{B}_{10}\text{H}_{10})]\text{RuH}(\text{PPh}_3)\}\{\text{K}(\text{DME})\}_2$. Treatment of $[\eta^5\text{-}\sigma\text{-Me}_2\text{C}(\text{C}_5\text{H}_4)(\text{C}_2\text{B}_{10}\text{H}_{10})]\text{RuH}_2(\text{PPh}_3)$ (**3**) with 2 equiv of KH in refluxing THF gave, after recrystallization from DME, an ionic complex $\{[\eta^5\text{-}\sigma\text{-Me}_2\text{C}(\text{C}_5\text{H}_4)(\text{C}_2\text{B}_{10}\text{H}_9)]\text{RuH}(\text{PPh}_3)\}\{\text{K}(\text{DME})\}_2$ (**7**) in 85% isolated yield (Scheme 3). The possible path way for the formation of **7** may include the reductive elimination of **3** upon heating with liberation of H_2 ,

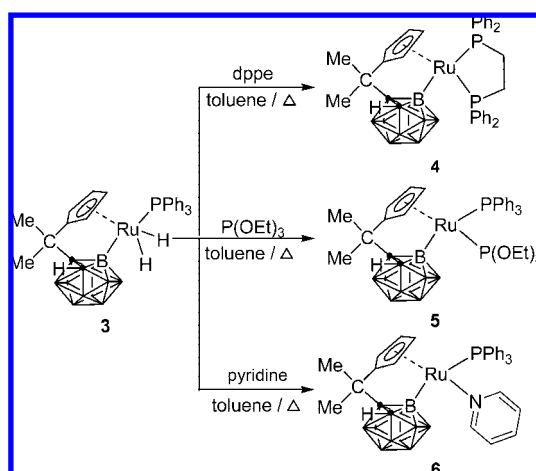
Table 1. Selected Bond Lengths (Å) and Angles (deg) for 2–7

	2	3	4	5	6	7
av. Ru–C _{ring}	2.249(2)	2.239(3)	2.259(6)	2.272(4)	2.228(2)	2.250(4)
Ru–B _{cage}	2.075(3)	2.087(3)	2.088(6)	2.128(4)	2.094(2)	2.018(5)
av. Ru–H	1.44(3)	1.53(3)				1.56(4)
Ru–Cent ^a	1.898	1.887	1.910	1.921	1.871	1.899
C(1)–C(2)	1.634(3)	1.633(4)	1.622(7)	1.646(6)	1.623(3)	1.597(5)
C(1)–B(3)	1.863(3)	1.858(4)	1.900(8)	1.898(5)	1.876(3)	1.969(6)
C(1)–B(4)	1.667(3)	1.687(4)	1.687(8)	1.642(6)	1.681(3)	1.743(6)
C(1)–B(5)	1.724(4)	1.718(4)	1.702(8)	1.736(6)	1.720(3)	1.726(6)
C(1)–B(6)	1.731(4)	1.721(4)	1.733(9)	1.745(6)	1.731(3)	1.725(6)
P–Ru–B _{cage}	111.5(1)	112.5(1)	92.8(2)	95.5(1)	94.4(1)	95.6(1)
Cent–Ru–B _{cage}	114.6	114.1	113.6	112.9	114.7	116.1
P(1)–Ru–P(2)			82.3(1)	95.2(1)	96.3(1) ^b	
C _{ring} –C _{bridge} –B _{cage}	109.0(2)	109.4(2)	109.1(4)	108.8(3)	108.8(2)	108.9(3)

^a Cent: the centroid of the cyclopentadienyl ring. ^b Angle of P–Ru–N.

Table 2. Crystal Data and Summary of Data Collection and Refinement for 2–7

	2 · 0.5C ₆ H ₆	3 · C ₆ H ₆	4	5	6	7
formula	C _{31.5} H ₅₉ B ₁₀ PRu	C ₃₄ H ₄₃ B ₁₀ PRu	C ₃₆ H ₄₄ B ₁₀ P ₂ Ru	C ₃₄ H ₅₀ B ₁₀ O ₃ P ₂ Ru	C ₃₃ H ₄₀ B ₁₀ NPRu	C ₆₄ H ₉₂ B ₂₀ K ₂ O ₄ P ₂ Ru ₂
cryst size (mm)	0.50 × 0.40 × 0.20	0.50 × 0.40 × 0.30	0.50 × 0.40 × 0.30	0.30 × 0.20 × 0.10	0.40 × 0.30 × 0.20	0.40 × 0.30 × 0.20
fw	677.9	691.8	747.8	777.8	690.8	1483.9
cryst syst	triclinic	monoclinic	monoclinic	monoclinic	triclinic	triclinic
space group	<i>P</i> (−1)	<i>P</i> 2 ₁ / <i>n</i>	<i>P</i> 2 ₁	<i>P</i> 2 ₁ / <i>n</i>	<i>P</i> (−1)	<i>P</i> (−1)
<i>a</i> , Å	9.913(1)	9.291(1)	9.153(2)	10.750(2)	10.434(1)	11.304(2)
<i>b</i> , Å	12.582(1)	26.196(2)	17.736(4)	20.386(4)	10.750(1)	12.737(4)
<i>c</i> , Å	15.460(1)	4.601(1)	11.175(2)	18.477(4)	15.093(2)	14.163(2)
α, deg	97.57(1)	90	90	90	97.23(1)	77.41(1)
β, deg	98.19(1)	93.20(1)	90.96(3)	102.82(3)	90.23(1)	68.63(1)
γ, deg	110.54(1)	90	90	90	92.51(1)	78.16(1)
<i>V</i> , Å ³	1752.5(2)	3548.3(5)	1813.8(6)	3948.5(1)	1677.8(3)	1835.6(4)
<i>Z</i>	2	4	2	4	2	1
<i>D</i> _{calcd} , Mg/m ³	1.285	1.295	1.369	1.309	1.367	1.342
radiation (λ), Å	Mo Kα (0.71073)	Mo Kα (0.71073)	Mo Kα (0.71073)	Mo Kα (0.71073)	Mo Kα (0.71073)	Mo Kα (0.71073)
2θ range, deg	2.7 to 50.0	3.1 to 56.0	4.4 to 50.0	3.1 to 51.0	4.0 to 56.0	3.1 to 50.0
μ, mm ^{−1}	0.515	0.511	0.548	0.511	0.541	0.613
<i>F</i> (000)	714	1424	768	1608	764	764
no. of obsd	6113	8548	3514	6485	7959	6434
no. of params	414	423	442	451	415	428
goodness of fit	1.014	1.043	1.024	1.097	1.050	1.030
<i>R</i> 1	0.029	0.039	0.031	0.047	0.030	0.042
<i>wR</i> 2	0.081	0.096	0.078	0.126	0.074	0.094

Scheme 2

followed by reaction with KH.²³ This result suggested that KH is not strong enough to deprotonate the cage CH proton.

The ¹H NMR spectrum of 7 showed four multiplets at 5.46, 5.00, 4.80, and 4.21 ppm assignable to the Cp protons, one broad singlet at 3.25 ppm corresponding to the cage CH proton, and one doublet at −11.75 ppm with ²*J*_{PH} = 30.0 Hz attributable to

the Ru–H proton in addition to the resonances of Me₂C-, DME, and PPh₃ groups. The ¹³C NMR spectrum is consistent with the ¹H NMR results. A pattern of 1:1:1:4:2 was observed in the ¹¹B{¹H} NMR spectrum. Its ³¹P NMR spectrum displayed one signal at 77.6 ppm.

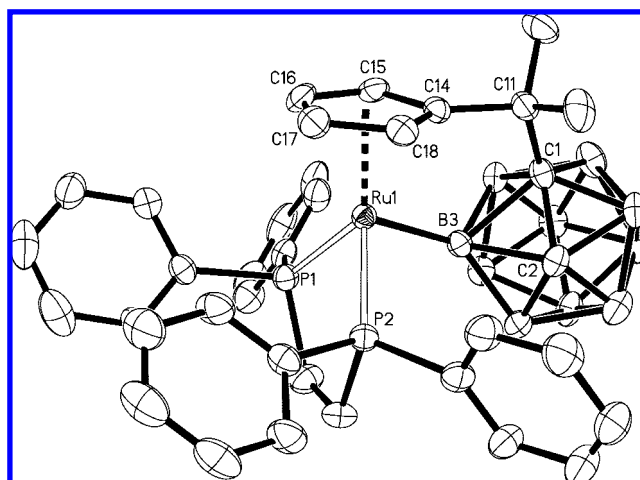


Figure 3. Molecular structure of [η⁵:σ_B-Me₂C(C₅H₄)(C₂B₁₀H₁₀)]Ru(dppe) (4) (thermal ellipsoids drawn at the 30% probability level).

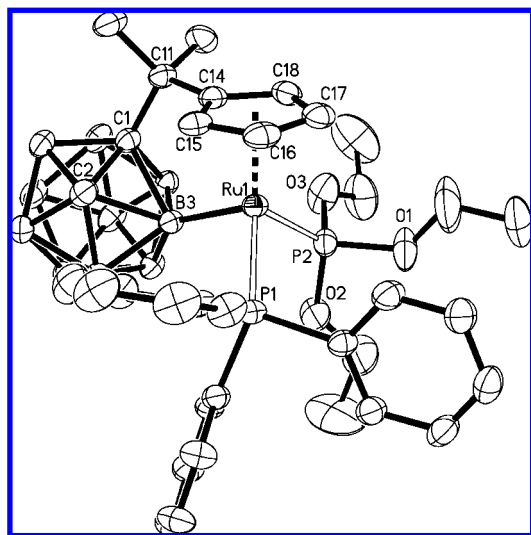


Figure 4. Molecular structure of the anion in $[\eta^5\text{-}\sigma_{\text{B}}\text{-Me}_2\text{C}(\text{C}_5\text{H}_4)\text{-(C}_2\text{B}_{10}\text{H}_{10})]\text{Ru}(\text{PPh}_3)(\text{P}(\text{OEt})_3)$ (**5**) (thermal ellipsoids drawn at the 30% probability level).

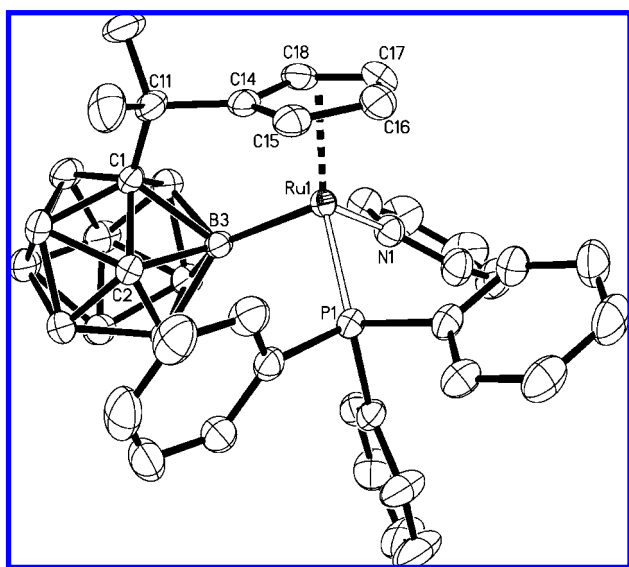
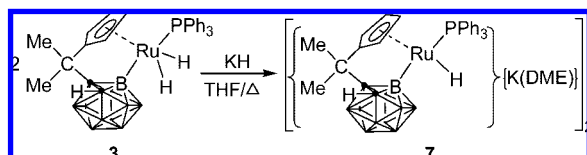


Figure 5. Molecular structure of $[\eta^5\text{-}\sigma_{\text{B}}\text{-Me}_2\text{C}(\text{C}_5\text{H}_4)\text{-(C}_2\text{B}_{10}\text{H}_{10})]\text{Ru}(\text{PPh}_3)(\text{Py})$ (**6**) (thermal ellipsoids drawn at the 30% probability level).

Scheme 3



Single-crystal X-ray diffraction study revealed that **7** is a centrosymmetric dimer with an inversion center at the midpoint of the $\text{K}(1)\text{--K}(1\text{A})$ connectivity. Each Ru atom is η^5 -bound to the cyclopentadienyl ring, σ -bound to the cage boron atom and one doubly bridging hydrogen atom, and coordinated to one PPh_3 in a three-legged piano stool geometry (Figure 6). The average $\text{Ru--C}(\text{ring})/\text{Ru--H}$ distances of 2.250(4)/1.56(4) Å and $\text{C}_{\text{ring}}\text{--C}_{\text{bridge}}\text{--B}_{\text{cage}}$ angle of 108.9(3)° are similar to the corresponding values of 2.239(3)/1.53(3) Å and 109.4(2)° observed

in **3**. The $\text{Ru--B}(\text{cage})$ distance of 2.018(5) Å is comparable to that of 2.087(3) Å in **3**.

Reaction Pathway/Density Functional Theory (DFT) Calculations. The above conversion from the metal–carbon to metal–boron bond in metal–carboranyl complexes, shown in Scheme 1, is totally unexpected, and similar reactions have never been observed before. To better understand the conversion process, we carried out DFT calculations. It is reasonably assumed that the initial event for the conversion is a simple ligand substitution of COD by H_2/PR_3 ($\text{R} = \text{Cy}$ or Ph) leading to the formation of a ruthenium dihydride intermediate (**A**), from which a metal–carbon to metal–boron conversion then occurs to give **2** or **3** (Scheme 4). Our DFT calculations based on PMe_3 models indeed indicate that the simple ligand substitution is thermodynamically favorable (Scheme 5).

Figure 7 shows the energy profile calculated for the conversion from the metal–carbon bonded intermediate **A** to the metal–boron bonded species **B'** and then to its more stable trans isomer **B**, a model complex for **2** or **3**. It can be seen that the conversion is both kinetically and thermodynamically favorable. The conversion is a one-step process assisted by one of the two hydride ligands, in which B--H bond breaking and C--H bond forming occur simultaneously.

The result that the metal–boron bonded isomer **B** is thermodynamically more stable than the metal–carbon bonded isomer **A** is quite unexpected in view of the fact that M--C σ -bonded metal–carboranyl complexes are far more prevalent than the M--B σ -bonded metal–carboranyl complexes. The findings here have the following important implication. The prevalent M--C σ -bonded metal–carboranyl complexes reported in the literature are likely kinetic products. They normally do not undergo isomerization to the thermodynamically more stable M--B σ -bonded metal–carboranyl complexes, due to a kinetic reason. In the absence of a hydride ligand, very high barriers for the isomerization are clearly expected.

Experimentally, it was also found that liberation of dihydrogen in **2** and **3** readily occurred in the presence of coordination ligands (Scheme 2). Our DFT calculation results show that the ligand substitution is indeed thermodynamically favorable (Scheme 6).

Conclusion

An unexpected hydrogen-mediated Ru--C to Ru--B bond conversion is observed in metal–carboranyl complexes for the first time. In the absence of dihydrogen, $[\eta^5\text{-}\sigma_{\text{C}}\text{-Me}_2\text{C}(\text{C}_5\text{H}_4)\text{-(C}_2\text{B}_{10}\text{H}_{10})]\text{Ru}(\text{COD})$ is very thermally stable. Dihydrogen is the promoter of this transformation. Such a process leads to a change in molecular symmetry, resulting in significantly different patterns in NMR spectra between two metal–carboranyl isomers containing either M--C or M--B bonds, although they have very similar solid-state structures. DFT calculations show such a conversion is both kinetically and thermodynamically favorable and a hydride ligand is crucial to the conversion.

Experimental Section

General Procedures. All experiments were performed under an atmosphere of dry nitrogen with the rigid exclusion of air and moisture using standard Schlenk or cannula techniques, or in a glovebox. All organic solvents were freshly distilled from sodium benzophenone ketyl immediately prior to use. $[\eta^5\text{-}\sigma_{\text{C}}\text{-Me}_2\text{C}(\text{C}_5\text{H}_4)\text{-(C}_2\text{B}_{10}\text{H}_{10})]\text{Ru}(\text{COD})$ was prepared according to literature method.¹²

(23) For the reaction of $\text{Ru}_3(\text{CO})_{12}$ with KH, see: Bricker, J. C.; Payne, M. W.; Shore, S. G. *Organometallics* **1987**, *6*, 2545.

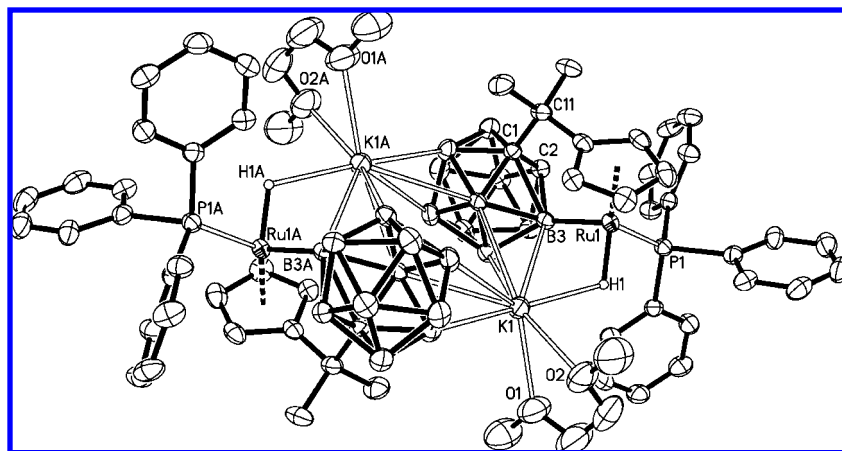
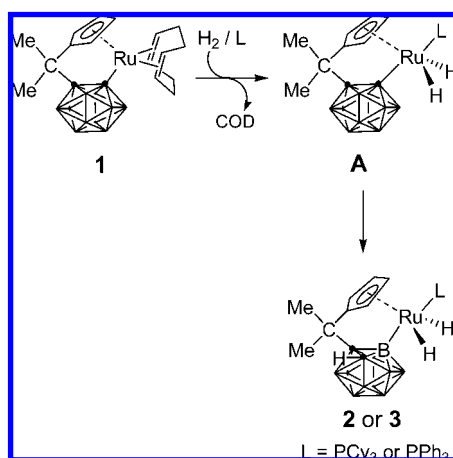
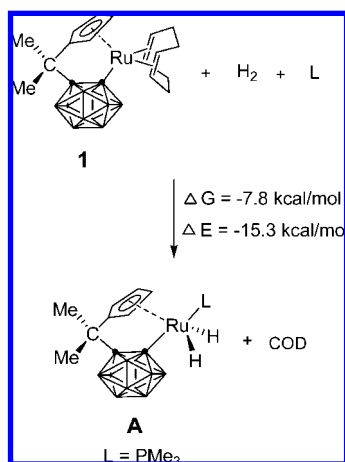


Figure 6. Molecular structure of $[[\eta^5\text{-}\sigma_{\text{B}}\text{-Me}_2\text{C}(\text{C}_5\text{H}_4)(\text{C}_2\text{B}_{10}\text{H}_{10})]\text{RuH}(\text{PPh}_3)]\{\text{K}(\text{DME})\}_2$ (**7**) (thermal ellipsoids drawn at the 30% probability level).

Scheme 4



Scheme 5



All other chemicals were purchased from either Aldrich or Acros Chemical Co. and used as received unless otherwise noted. Infrared spectra were obtained from KBr pellets prepared in the glovebox on a Perkin-Elmer 1600 Fourier transform spectrometer. ^1H and ^{13}C NMR spectra were recorded on a Bruker DPX 300 spectrometer at 300.0 and 75.5 MHz, respectively. ^{11}B and ^{31}P NMR spectra were recorded on a Varian Inova 400 spectrometer at 128.0 and 162.0 MHz. All chemical shifts were reported in δ units with references to the residual protons of the deuterated solvents for proton and carbon chemical shifts, to external $\text{BF}_3 \cdot \text{OEt}_2$ (0.00 ppm) for boron chemical shifts, and to external 85% H_3PO_4 (0.00 ppm)

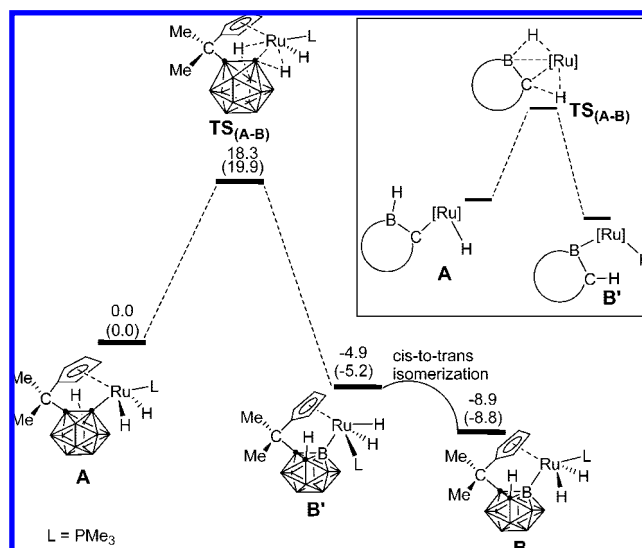


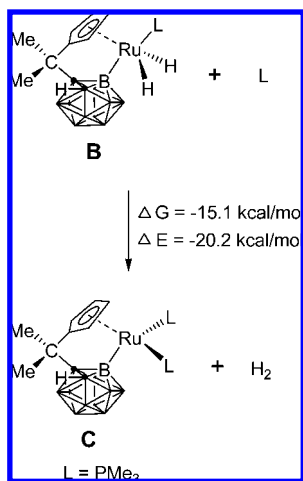
Figure 7. Energy profile calculated for the conversion of the model complex **A** to **B**. A schematic illustration of the bond breaking and forming process is given in the pane window on the upper-right side. The calculated relative energies and electronic energies (in parentheses) are given in kcal/mol.

for phosphorus chemical shifts. Elemental analyses were performed by MEDAC Ltd., Middlesex, U.K.

Preparation of $[\eta^5\text{-}\sigma_{\text{B}}\text{-Me}_2\text{C}(\text{C}_5\text{H}_4)(\text{C}_2\text{B}_{10}\text{H}_{10})]\text{RuH}_2(\text{PCy}_3)$ (2**).**

A Schlenk flask with a Teflon valve was charged with $[\eta^5\text{-}\sigma_{\text{C}}\text{-Me}_2\text{C}(\text{C}_5\text{H}_4)(\text{C}_2\text{B}_{10}\text{H}_{10})]\text{Ru}(\text{COD})$ (**1**; 0.23 g, 0.50 mmol), PCy_3 (0.14 g, 0.50 mmol), THF (10 mL), and dihydrogen. The flask was closed and heated at 60 °C for 12 h until the color of the solution was changed from brown to pale yellow. After removal of THF, the residue was washed with *n*-hexane. Recrystallization from a THF/toluene solution gave **2** (0.5 toluene) as almost colorless crystals (0.28 g, 88%): ^1H NMR (C_6D_6) δ 5.26 (m, 1H), 4.84 (m, 1H), 4.67 (m, 1H), 4.53 (m, 1H) (C_5H_4), 3.30 (s, 1H) (cage CH), 1.94–0.91 (m, 39H) ($\text{C}(\text{CH}_3)_2 + \text{Cy}$), –10.58 (dd, 2H, $^2J_{\text{PH}} = 30.0$ Hz, $^2J_{\text{HH}} = 3.0$ Hz) (Ru–H₂); $^{13}\text{C}\{^1\text{H}\}$ NMR (C_6D_6) δ 84.6, 83.7, 82.5, 82.2 (C_5H_4), 65.1 (cage C), 40.1 ($\text{C}(\text{CH}_3)_2$), 39.4 (d, $^1J_{\text{CP}} = 31.5$ Hz), 32.0 (d, $^2J_{\text{CP}} = 9.4$ Hz), 31.5, 30.3, 27.9, 27.1 (PCy + $\text{C}(\text{CH}_3)_2$); $^{31}\text{P}\{^1\text{H}\}$ NMR (C_6D_6) δ 82.2; ^{11}B NMR (C_6D_6) δ 11.2 (s, 1B), –1.8 (d, $J = 147$ Hz, 1B), –4.0 (d, $J = 133$ Hz, 1B), –7.0 (d, $J = 151$ Hz, 2B), –9.6 (d, $J = 159$ Hz, 2B), –10.7 (d, $J = 140$ Hz, 2B), –14.4 (d, $J = 156$ Hz, 1B); IR (KBr, cm^{-1}) ν 2576 (vs) (B–H), 1958 (m) (Ru–H). Anal. Calcd for $\text{C}_{28}\text{H}_{55}\text{B}_{10}\text{PRu}$ (**2**): C, 53.22; H, 8.77. Found: C, 52.80; H, 8.45.

Scheme 6



Preparation of $[\eta^5\text{-}\sigma_{\text{B}}\text{-Me}_2\text{C}(\text{C}_5\text{H}_4)(\text{C}_2\text{B}_{10}\text{H}_{10})\text{RuH}_2(\text{PPh}_3)]$ (**3**).

This complex was prepared as almost colorless crystals from $[\eta^5\text{-}\sigma_{\text{C}}\text{-Me}_2\text{C}(\text{C}_5\text{H}_4)(\text{C}_2\text{B}_{10}\text{H}_{10})\text{Ru}(\text{COD})]$ (**1**; 0.23 g, 0.50 mmol), PPh₃ (0.13 g, 0.50 mmol), THF (10 mL), and dihydrogen using the same procedures reported for **2**: yield 0.30 g (87%). Single crystals of **3**·C₆H₆ suitable for X-ray analyses were grown from a benzene solution: ¹H NMR (C₆D₆) δ 7.63 (m, 6H), 7.09 (m, 9H) (aryl H), 5.21 (m, 1H), 4.87 (m, 1H), 4.40 (m, 1H), 4.18 (m, 1H) (C₅H₄), 3.20 (s, 1H) (cage CH), 1.25 (s, 3H), 0.84 (s, 3H) (C(CH₃)₂), -9.60 (dd, 2H, ²J_{PH} = 30.0 Hz, ²J_{HH} = 3.0 Hz) (Ru-H₂); ¹³C{¹H} NMR (C₆D₆) δ 139.6 (d, ¹J_{CP} = 49.7 Hz), 133.6 (d, ²J_{CP} = 11.4 Hz), 129.8, 117.4 (aryl C), 85.3, 85.1, 84.1 (C₅H₄), 64.9 (cage C), 40.0 (C(CH₃)₂), 32.3, 29.6 (C(CH₃)₂); ³¹P{¹H} NMR (C₆D₆) δ 63.3; ¹¹B NMR (C₆D₆) δ 9.6 (s, 1B), -1.8 (d, J = 138 Hz, 1B), -3.6 (d, J = 145 Hz, 1B), -6.5 (d, J = 126 Hz, 1B), -10.3 (d, J = 137 Hz, 2B), -10.8 (d, J = 110 Hz, 3B), -13.8 (d, J = 133 Hz, 1B); IR (KBr, cm⁻¹) ν 2582 (vs) (B-H), 1990 (m) (Ru-H). Anal. Calcd for C₃₄H₄₃B₁₀PRu (**3** + C₆H₆): C, 59.03; H, 6.26. Found: C, 58.84; H, 5.78.

Preparation of $[\eta^5\text{-}\sigma_{\text{B}}\text{-Me}_2\text{C}(\text{C}_5\text{H}_4)(\text{C}_2\text{B}_{10}\text{H}_{10})\text{Ru}(\text{dppe})]$ (**4**).

A toluene solution (15 mL) of $[\eta^5\text{-}\sigma_{\text{B}}\text{-Me}_2\text{C}(\text{C}_5\text{H}_4)(\text{C}_2\text{B}_{10}\text{H}_{10})\text{RuH}_2(\text{PPh}_3)]$ (**3**; 0.32 g, 0.50 mmol) and dppe (0.20 g, 0.50 mmol) was heated to reflux for 5 days. After removal of toluene, the residue was washed with hexane (10 mL). Recrystallization from a CH₂Cl₂ solution gave **4** as yellow crystals (0.30 g, 80%): ¹H NMR (CDCl₃) δ 7.86–6.96 (m, 20H) (aryl H), 5.46 (m, 1H), 5.28 (m, 1H), 5.19 (m, 1H), 4.53 (m, 1H) (C₅H₄), 2.35 (s, 1H) (cage CH), 2.77 (m, 2H), 2.10 (m, 2H) (CH₂CH₂), 1.49 (s, 3H), 1.15 (s, 3H) (C(CH₃)₂); ¹³C{¹H} NMR (CDCl₃) δ 132.7 (d, ¹J_{CP} = 37.6 Hz), 132.5 (d, ¹J_{CP} = 40.4 Hz), 132.2, 131.1 (d, ²J_{CP} = 10.5 Hz), 129.5, 128.3 (d, ²J_{CP} = 9.0 Hz), 128.1, 127.6 (aryl C), 90.8, 81.5, 78.9, 75.6 (C₅H₄), 68.3, 61.7 (cage C), 41.1 (C(CH₃)₂), 33.8, 28.6 (C(CH₃)₂), 25.9 (t, ¹J_{CP} = 35.4 Hz) (CH₂CH₂); ³¹P{¹H} NMR (CDCl₃) δ 89.3, 87.6; ¹¹B NMR (CDCl₃) δ 15.0 (s, 1B), -2.7 (d, J = 136 Hz, 1B), -4.4 (d, J = 135 Hz, 1B), -8.6 (d, J = 157 Hz, 2B), -10.0 (d, J = 133 Hz, 3B), -12.4 (d, J = 132 Hz, 1B), -14.7 (d, J = 155 Hz, 1B); IR (KBr) ν_{BH} 2563 (s) cm⁻¹. Anal. Calcd for C₃₆H₄₄B₁₀P₂Ru (**4**): C, 57.82; H, 5.93. Found: C, 57.70; H, 5.79.

Preparation of $[\eta^5\text{-}\sigma_{\text{B}}\text{-Me}_2\text{C}(\text{C}_5\text{H}_4)(\text{C}_2\text{B}_{10}\text{H}_{10})\text{Ru}(\text{PPh}_3)[\text{P}(\text{OEt})_3]$ (**5**).

Triethyl phosphate (0.17 g, 1.00 mmol) was added to a toluene solution (10 mL) of $[\eta^5\text{-}\sigma_{\text{B}}\text{-Me}_2\text{C}(\text{C}_5\text{H}_4)(\text{C}_2\text{B}_{10}\text{H}_{10})\text{RuH}_2(\text{PPh}_3)]$ (**3**; 0.32 g, 0.50 mmol), and the mixture was heated to reflux for 12 h. After removal of the solvent, the residue was washed with hexane and recrystallized from CH₂Cl₂ at room temperature to give **5** as pale yellow crystals (0.30 g, 77%): ¹H NMR (CDCl₃) δ 7.42–7.27 (m, 15H) (aryl H), 4.79 (m, 1H), 4.65 (m, 1H), 4.43 (m, 1H), 3.99 (m, 1H) (C₅H₄), 3.73 (m, 6H) (OCH₂), 3.12 (s, 1H) (cage CH), 1.45 (s, 3H), 1.23 (s, 3H) (C(CH₃)₂), 1.09 (t, ³J = 6.9 Hz, 9H) (CH₂CH₃); ¹³C{¹H} NMR (CDCl₃) δ 134.2 (d, ¹J_{CP} = 35.4 Hz),

129.0, 127.4 (d, ²J_{CP} = 9.2 Hz), 123.0 (aryl C), 81.1, 77.4, 77.3, 76.7 (C₅H₄), 63.0 (cage C), 60.6 (d, ²J_{CP} = 9.2 Hz, OCH₂), 40.6 (C(CH₃)₂), 33.8, 27.7 (C(CH₃)₂), 15.9 (CH₂CH₃); ³¹P{¹H} NMR (CDCl₃) δ 145.0 (d, ²J_{PP} = 68.4 Hz, 1P), 54.5 (d, ²J_{PP} = 68.4 Hz, 1P); ¹¹B NMR (CDCl₃) δ 15.6 (s, 1B), -3.2 (d, J = 171 Hz, 1B), -4.6 (d, J = 147 Hz, 1B), -7.9 (d, J = 143 Hz, 1B), -10.6 (d, J = 141 Hz, 3B), -12.0 (d, J = 133 Hz, 2B), -15.0 (d, J = 151 Hz, 1B); IR (KBr, cm⁻¹) ν 2533 (vs) (B-H). Anal. Calcd for C₃₄H₅₀B₁₀O₃P₂Ru (**5**): C, 52.50; H, 6.48. Found: C, 52.78; H, 6.17.

Preparation of $[\eta^5\text{-}\sigma_{\text{B}}\text{-Me}_2\text{C}(\text{C}_5\text{H}_4)(\text{C}_2\text{B}_{10}\text{H}_{10})\text{Ru}(\text{PPh}_3)(\text{Py})]$ (**6**).

Pyridine (0.08 g, 1.00 mmol) was added to a toluene solution (10 mL) of $[\eta^5\text{-}\sigma_{\text{B}}\text{-Me}_2\text{C}(\text{C}_5\text{H}_4)(\text{C}_2\text{B}_{10}\text{H}_{10})\text{RuH}_2(\text{PPh}_3)]$ (**3**; 0.32 g, 0.50 mmol), and the mixture was heated to reflux for 2 days. After removal of the solvent, the residue was washed with hexane and recrystallized from DME at room temperature to give **6** as pale yellow crystals (0.28 g, 81%): ¹H NMR (benzene-*d*₆) δ 9.10 (m, 2H), 6.59 (m, 1H), 6.05 (m, 2H) (C₅H₅N), 7.56 (m, 6H), 6.99 (m, 9H) (aryl H), 4.57 (m, 1H), 4.39 (m, 2H), 3.35 (m, 1H) (C₅H₄), 2.52 (s, 1H) (cage CH), 1.46 (s, 3H), 0.79 (s, 3H) (C(CH₃)₂); ¹³C{¹H} NMR (benzene-*d*₆) δ 159.2, 135.2, 134.5, 129.4 (d, ¹J_{CP} = 31.3 Hz), 127.7 (d, ²J_{CP} = 8.0 Hz), 122.9, 117.3 (aryl C), 93.6, 89.3, 73.1, 72.9 (C₅H₄), 63.7, 61.6 (cage C), 41.7 (C(CH₃)₂), 33.8, 28.9 (C(CH₃)₂); ³¹P{¹H} NMR (benzene-*d*₆) δ 66.9; ¹¹B NMR (benzene-*d*₆) δ 18.2 (1B), -2.2 (d, J = 159 Hz, 1B), -4.3 (d, J = 149 Hz, 2B), -9.6 (d, J = 132 Hz, 3B), -11.4 (d, J = 160 Hz, 2B), -14.6 (d, J = 148 Hz, 1B); IR (KBr, cm⁻¹) ν 2557 (vs) (B-H). Anal. Calcd for C₃₃H₄₀B₁₀NPRu (**6**): C, 57.37; H, 5.84; N, 2.03. Found: C, 57.55; H, 5.64; N, 1.76.

Preparation of $\{[\eta^5\text{-}\sigma_{\text{B}}\text{-Me}_2\text{C}(\text{C}_5\text{H}_4)(\text{C}_2\text{B}_{10}\text{H}_{10})\text{RuH}(\text{PPh}_3)]\text{-K}(\text{DME})\}_2$ (**7**).

To a THF (10 mL) solution of $[\eta^5\text{-}\sigma_{\text{B}}\text{-Me}_2\text{C}(\text{C}_5\text{H}_4)(\text{C}_2\text{B}_{10}\text{H}_{10})\text{RuH}_2(\text{PPh}_3)]$ (**3**; 0.32 g, 0.50 mmol) was added KH powder (0.04 g, 1.00 mmol), and the mixture was then heated to reflux for 3 days. After filtration and removal of THF, the residue was recrystallized from DME to give **7** as yellow crystals (0.32 g, 85%): ¹H NMR (pyridine-*d*₅) δ 8.17 (m, 6H), 7.25 (m, 9H) (aryl H), 5.46 (m, 1H), 5.00 (m, 1H), 4.80 (m, 1H), 4.21 (m, 1H) (C₅H₄), 3.48 (s, 5H), 3.25 (s, 6H) (DME + cage CH), 1.64 (s, 3H), 1.34 (s, 3H) (C(CH₃)₂), -11.75 (d, ²J_{PH} = 30.0 Hz, 1H) (Ru-H); ¹³C{¹H} NMR (pyridine-*d*₅) δ 134.9 (d, ¹J_{CP} = 22.5 Hz), 129.4, 127.8, 127.3 (d, ²J_{CP} = 8.3 Hz) (aryl C), 87.5, 85.5, 79.7, 77.8, 76.9 (C₅H₄), 64.5 (cage C), 68.2, 66.1 (DME), 40.9 (C(CH₃)₂), 33.8, 30.7 (C(CH₃)₂); ³¹P{¹H} NMR (pyridine-*d*₅) δ 77.8; ¹¹B NMR (pyridine-*d*₅) δ -4.4 (d, J = 157 Hz, 1B), -6.4 (d, J = 168 Hz, 1B), -9.1 (d, J = 150 Hz, 1B), -11.5 (d, J = 178 Hz, 3B), -19.7 (d, J = 134 Hz, 3B), -43.1 (s, 1B); IR (KBr, cm⁻¹) ν 2572 (vs) (B-H). Anal. Calcd for C₆₄H₉₂B₂₀K₂O₄P₂Ru₂ (**7**): C, 51.80; H, 6.25. Found: C, 52.21; H, 6.25.

X-ray Structure Determination. All single crystals were immersed in Paraton-N oil and sealed under nitrogen in thin-walled glass capillaries. Data were collected at 293 K on a Bruker SMART 1000 CCD diffractometer using Mo Kα radiation. An empirical absorption correction was applied using the SADABS program.²⁴ All structures were solved by direct methods and subsequent Fourier difference techniques and refined anisotropically for all non-hydrogen atoms by full-matrix least-squares on F² using the SHELXTL program package.²⁵ For the noncentrosymmetric structure of **4**, the appropriate enantiomorph was chosen by refining Flack's parameter *x* toward zero.²⁶ The cage carbon atoms were located by comparing the bond lengths as the average distance between the carbon and carbon/boron atoms would appear shorter than that between the boron atoms. All hydrogen atoms were geometrically fixed using the riding model. Complexes **2** and **3** showed the solvation of half

(24) Sheldrick, G. M. *SADABS: Program for Empirical Absorption Correction of Area Detector Data*; University of Göttingen: Göttingen, Germany, 1996.

(25) Sheldrick, G. M. *SHELXTL 5.10 for Windows NT: Structure Determination Software Programs*; Bruker Analytical X-ray systems, Inc.: Madison, WI, 1997.

(26) Flack, H. D. *Acta Crystallogr.* **1983**, A39, 876.

toluene and one benzene. Crystal data and details of data collection and structure refinements are given in Table 2. Further details are included in the Supporting Information.

Computational Details. Full geometry optimizations of all the model complexes were done at the Becke3LYP (B3LYP) level of density functional theory (DFT).²⁷ Frequency calculations had also been performed at the same level of theory to identify all the stationary points as minima (zero imaginary frequency) or transition states (one imaginary frequency) and to provide free energy at 298.15 K, which include entropic contributions by taking into account the vibrational, rotational, and translational motions of the species under consideration. Transition states were located using the Berny algorithm. Intrinsic reaction coordinates (IRC)²⁸ were calculated for the transition states to confirm that such structures

are indeed connecting two relevant minima. The effective core potentials (ECPs) of Hay and Wadt with double- ζ valence basis sets (LanL2DZ)²⁹ were used to describe Ru and P. Polarization functions were also added for Ru ($\zeta_r = 1.235$) and P ($\zeta_d = 0.387$).³⁰ The 6-31G basis set was used for all the other atoms.³¹ All the calculations were performed with the Gaussian03 software package.³²

Acknowledgment. This work was supported by grants from the Research Grants Council of The Hong Kong Special Administration Region (Project No. 403906 to Z.X. and HKUST 601507 to Z.L.).

Supporting Information Available: Complete ref 32; crystallographic data in CIF format for **2**·0.5C₇H₈, **3**·C₆H₆, **4**, **5**, **6**, and **7**. This material is available free of charge via the Internet at <http://pubs.acs.org>.

JA8067098

- (27) (a) Becke, A. D. *Phys. Rev. A* **1988**, *38*, 3098. (b) Miehlich, B.; Savin, A.; Stoll, H.; Preuss, H. *Chem. Phys. Lett.* **1989**, *157*, 200. (c) Lee, C.; Yang, W.; Parr, G. *Phys. Rev. B* **1988**, *37*, 785.
- (28) (a) Fukui, K. *J. Phys. Chem.* **1970**, *74*, 4161. (b) Fukui, K. *Acc. Chem. Res.* **1981**, *14*, 363.
- (29) Hay, P. J.; Wadt, W. R. *J. Chem. Phys.* **1995**, *82*, 299.
- (30) (a) Ehlers, A. W.; Böhme, M.; Dapprich, S.; Gobbi, A.; Höllwarth, A.; Jonas, V.; Köhler, K. F.; Stegmann, R.; Veldkamp, A.; Frenking, G. *Chem. Phys. Lett.* **1993**, *208*, 111. (b) Höllwarth, A.; Böhme, M.; Dapprich, S.; Ehlers, A. W.; Obbi, A. G.; Jonas, V.; Köhler, K. F.; Stegmann, R.; Veldkamp, A.; Frenking, G. *Chem. Phys. Lett.* **1993**, *208*, 238.

- (31) (a) Gordon, M. S. *Chem. Phys. Lett.* **1980**, *76*, 163. (b) Hariharan, P. C.; Pople, J. A. *Theor. Chim. Acta* **1973**, *28*, 213. (c) Binning, R. C., Jr.; Curtiss, L. A. *J. Comput. Chem.* **1990**, *11*, 1206.
- (32) Frisch, M. J.; *Gaussian 03*, revision B05; Gaussian, Inc.: Pittsburgh, PA, 2003.